

Mid-IR Interferometric Nulling for TPF

J. Kent Wallace, Vivek Babiwale, Randy Bartos, Ken Brown, Robert Gappinger,
Frank Loya, Dan MacDonald, Stefan Martin, John Negron, Tuan Truong,
Gautam Vasisht

Jet Propulsion Laboratory, 4800 Oak Grove Dr. Pasadena, CA, 91109

ABSTRACT

By the middle of 2006, the Interferometry Technology development program for NASA's Terrestrial Planet Finder (TPF) Mission has the goal of demonstrating deep and stable interferometric nulling of broadband Mid-IR thermal radiation under conditions that are traceable to the expected on-orbit conditions. Specifically, the task is to demonstrate null levels of 10^{-6} , with a 50% BW centered at 10 μm , with null stabilities of 10^{-7} all at cryogenic temperatures for observational periods of a couple of hours. The Achromatic Nulling activity at JPL addresses this concern in two testbeds: the warm nulling testbed and the cryonulling testbed. The warm nulling testbed will demonstrate the physics of nulling broadband thermal sources in an environment that is conducive to efficient research. We'll explore nulling techniques, optical-mechanical alignment methods, motion control, and path-length metrology for a single beam interferometer, as well as preliminary planet detection techniques. Ultimate nulling capabilities under conditions that are more flight-like will be demonstrated in the cryogenic nulling testbed. Knowledge gained from operation at room temperature will be applied to the cryogenic experiment where we face the additional challenges of extreme temperatures, cryogenic actuators, component survivability and fluxes that are within an order of magnitude of expected flux levels on orbit. Concurrently, we will develop a low flux mid-IR camera that will allow us to measure the nulls at these faint photon fluxes. This talk will review this development activity and will include recent nulling experimental results and plans for future work.

Keywords: nulling, stellar interferometry, planet detection

1. INTRODUCTION

The direct detection of planets around nearby stars can succinctly be described as a task in the suppression of light from the host star relative to that of its companion. The challenges for the requisite angular resolution are modest: a telescope of diameter 30 cm, working in the visible, is capable of resolving, for instance, a Jupiter/Sun system at 10 pc. Existing space telescopes have also demonstrated the ability to measure very faint objects: Hubble for instance can detect objects as faint as 30th magnitude. It is the challenge of suppressing the flux from a nearby stellar companion that makes this a challenging effort.

Currently, two methods are seen as favorable, a coronagraph in the visible and nulling interferometry at a wavelength near 10 μm . This paper will describe the requirements that originate from an analysis of the proposed Mid-IR space interferometer, along with the time scales for their development. We then will describe our current progress on the experimental demonstration of these nulling techniques. We will subsequently detail our plans for the ultimate demonstration of nulling under conditions that closely approximate the anticipated on orbit conditions for the interferometer.

To place our nulling activities in the wider context of the TPF project, we need consider the requirements necessary for the final interferometer mission. The mission is currently envisioned as a multiple aperture system. The beams are combined to create a very deep, achromatic null fringe over the star of interest, thereby reducing the flux relative to the planet. A second null fringe is created which is used to modulate the light from the planet. This modulation serves to remove systematic errors of the interferometer and the exo-zodiacal light. One can consider the major challenges as twofold: the first is the creation of the null fringe, and the second is the system level requirements. This talk will discuss in detail the challenges of achromatic nulling interferometry. The system will need to demonstrate the ability to do achromatic nulling of 10^{-6} over a 50% BW at cryogenic temperatures, for long periods of time, with rudimentary

planet detection, and representative fluxes. Our approach to this ultimate goal is to first concentrate on a demonstration of deep and broad nulling at room temperature. This approach allows us to work on the challenges of nulling without the additional complications introduced by cryovac operation. We will be testing the challenges of the ultimate cryogenic nulling experiment by demonstrating key cryogenic nulling operations on a reduced scale. These tests will include a test of optical components and coatings, cryogenic actuation, mechanical mounting, and nulling operation.

Once the warm nulling and cryogenic tests are complete, we'll turn our full attention to the test of deep nulling over a broad band with rudimentary planet detection (two beam nulling vs. four) at cryogenic temperatures, with representative fluxes for long periods of time. This is called the cryogenic nulling testbed, (as opposed to cryogenic testing.)

Our near term efforts center upon the demonstration of room-temperature nulling and cryogenic testing. Our discussions will follow along these lines. In order to demonstrate these capabilities, we need to develop ancillary tools, which we'll describe in some detail. Finally, we'll describe our plans for the full-up demonstration.

2. WARM NULLING

2.1. Introduction to nulling architectures

In order to improve our odds of meeting the challenging requirements of broadband nulling at the 10⁻⁵ and 10⁻⁶ levels, we are pursuing three different nulling architectures. They are the phase plate field flip, the periscope field flip, and the through focus field flip. We have a range of previous experience for each from only initial results to years of experience from similar nullers in the visible. Each technique has its own distinct advantage; the definitive deciding factor between these different architectures will be the null depth that can be achieved. We will review each of these architectures noting their benefits, and drawbacks, a status of their performance, and a discussion of current performance.

2.2. Brief summary of nulling interferometry

In traditional interferometry, optical beams leave the source, and follow along two different paths until they are recombined again at the beam combining beamsplitter. Generally speaking, at the center of the coherent envelope, the fringe pattern internal to the envelope is at a maximum (assuming no differential dispersion between the two arms). We have a maximum of interference due to the simultaneous constructive coherent addition of the electric field vectors for each wavelength. The goal of a nulling interferometer is to create a situation whereby the electric field vectors are diametrically counter-posed, again broadband. If such a situation can be created, then at the center of the coherent envelope, there will be a null fringe that will be quite deep, approaching zero.

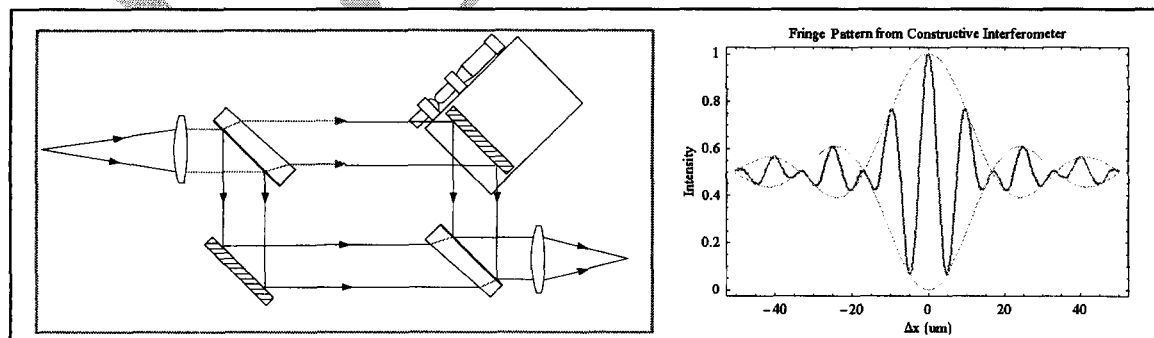


Fig. 1. A schematic of a constructive interferometer, and the output intensity as a function of path length difference.

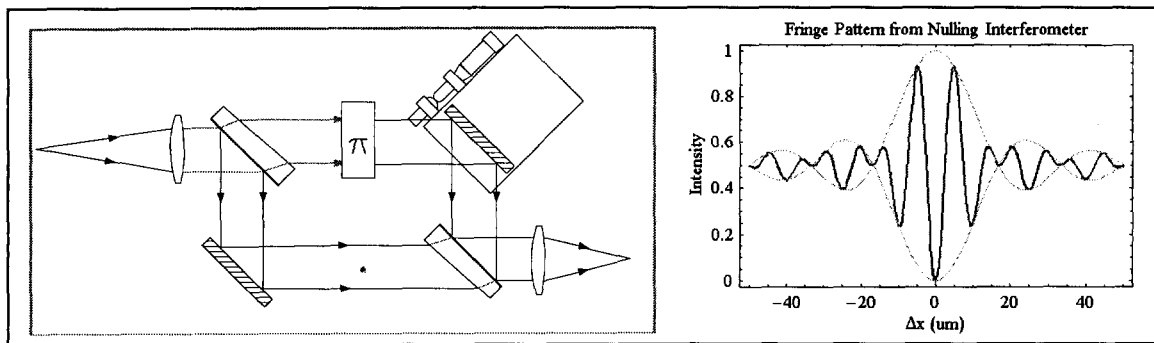


Fig. 2. A schematic of a nulling interferometer, and the output response as a function of path length difference.

2.3. Phase-Plate architecture

2.3.1. Discussion of the technique

For a single wavelength, the nulling condition can be accomplished by the introduction of a path delay difference between the two arms that results in a phase change of π . As the bandwidth is increased around this center wavelength, the wavelengths shorter will pick up a proportionally larger phase change, and longer wavelengths will pick up less than π phase change. Starting from this initial condition, it's possible to add an air delay in one arm while subtracting an equivalent amount of dielectric such that the phase at the center wavelength is still near π , while the next phase for wavelengths both shorter and longer have improved. This technique was initially proposed by Morgan, et.al. and was demonstrated in the visible. We have applied it to the mid-IR via a method they also proposed.

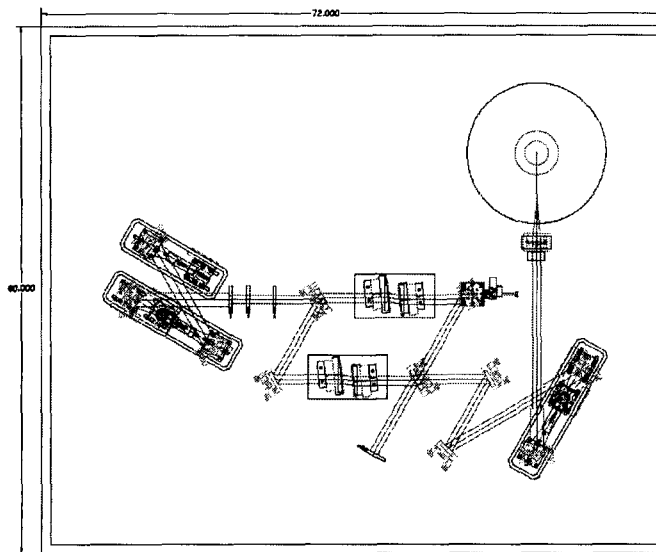
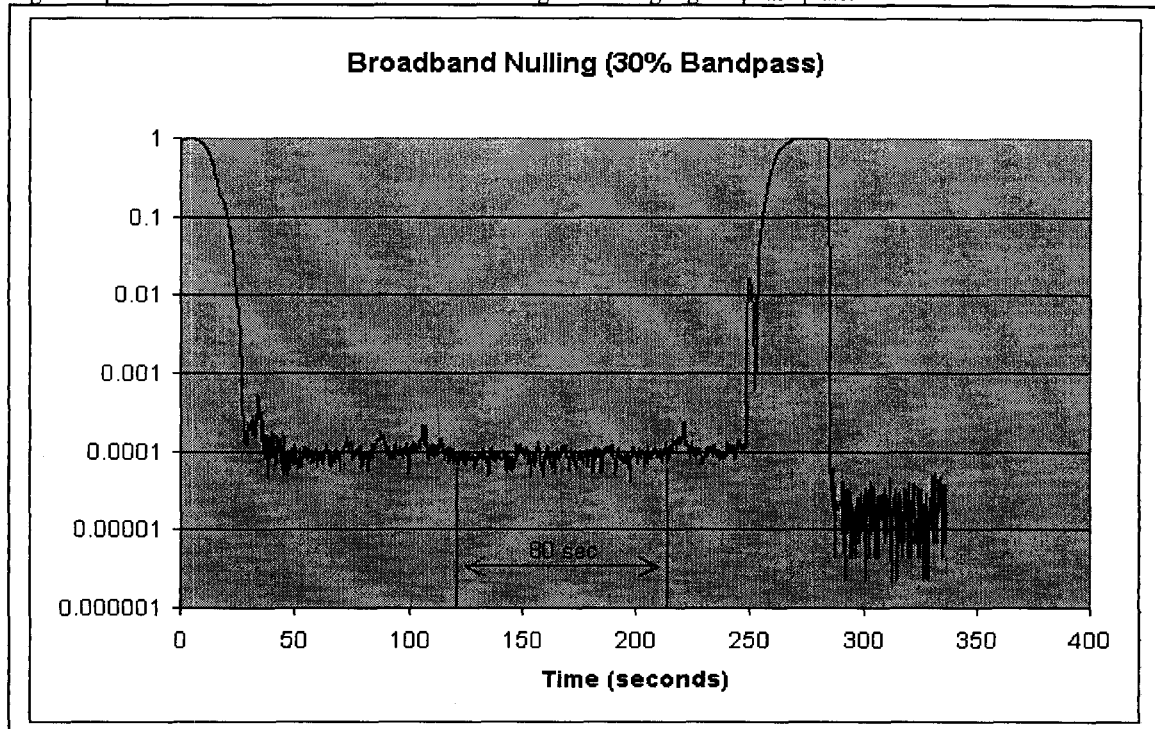


Fig. 3. Layout of a single-glass phase plate nulling interferometer.

2.3.2. Experimental results

For a single glass phase plate of ZnSe, and band pass of 30%, we have demonstrated a null depth of greater than 10^{-4} . Our theoretical prediction of null performance for the same optical bandwidth predict a null of $\sim 30,000:1$ if the residual dispersion is the single limiting factor.

Fig. 4. Experimental measurement of broadband nulling with a single-glass phase plate.



2.3.3. Future upgrades

We are in the process of moving to a two-glass solution. This will allow us to achieve a theoretical limit in null that is greater than 10^{-6} . These will replace the current single glass arrangement. The pieces are fabricated to near net thickness. Fine adjustments are made via a slight rotation of the substrate about an axis orthogonal to the plane of the interferometer.

2.3.4. Benefits/drawbacks of the phase-plate architecture

The benefits are its compact design and the non-inversion of the pupil. Each part of the pupil interferes with itself, so the effects of spatial coherence are negligible if the pupil shear and rotation are well controlled. Tolerances on the differential thickness are tight, and the limited knowledge of the index of refraction may be our limiting factor. Ghost reflections from the surfaces may also present an unacceptable level of background photons.

2.4. Through-Focus field flip

2.4.1. Discussion of the technique

Whereas the phase plate technique introduced a phase delay by introducing compensating dispersions, the through focus field flip can be thought of as a geometric effect. By putting the light through focus, the beam acquires an achromatic field flip. This technique was first proposed and demonstrated by Jean Gay, et.al. with an instrument having the clever acronym CIA (coronagraphe interferential achromatique).

2.4.2. Experiment Description

Our implementation of this technique is illustrated in Fig. 5, below. We include a pair of additional phase plates of the same material as the beamsplitters. These phase plates can be adjusted to remove the residual dispersion effects due to thickness mismatches between the split and beam recombination beamsplitters.

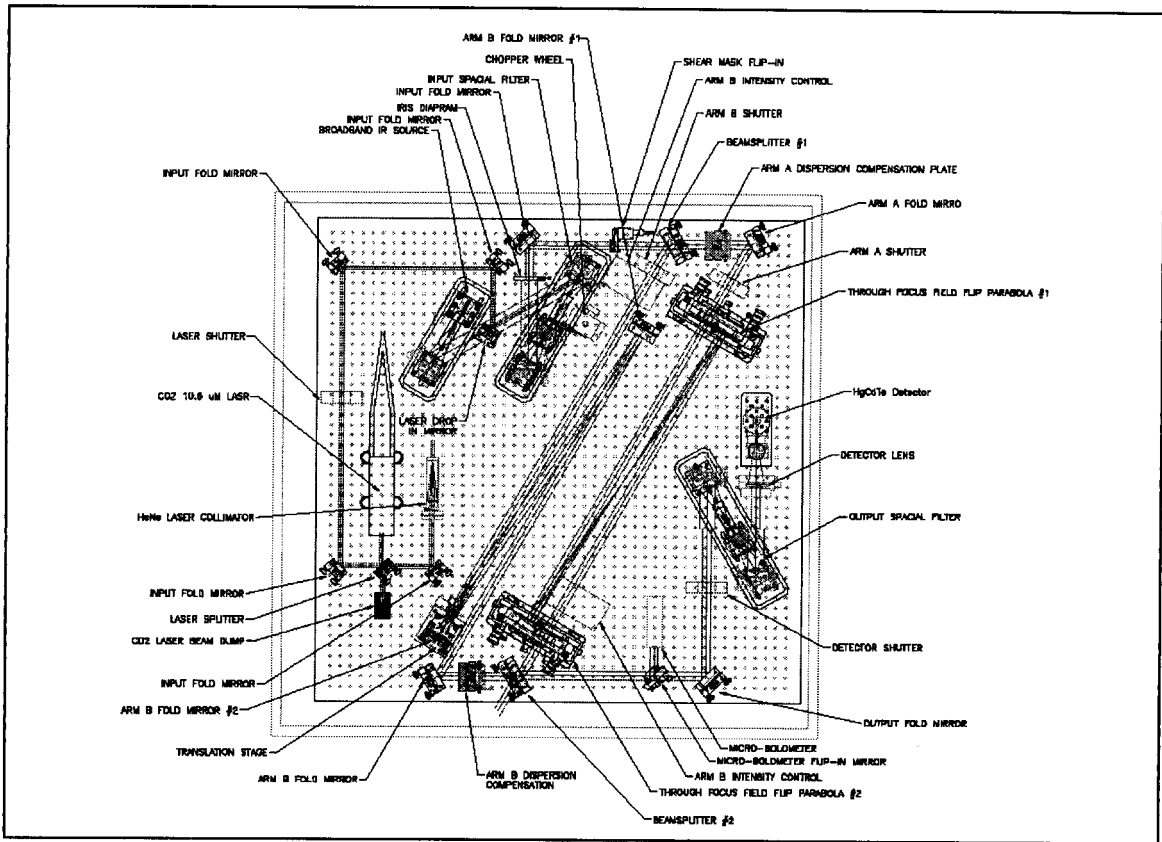


Fig. 5. Layout of the through-focus field flip architecture.

2.4.3. Experimental Results

Our preliminary results from this arrangement are shown below for a bandwidth of roughly 20%. We are working with a pair of parabolas that are not well matched. Likewise, our current setup uses a pinhole spatial filter for both the input and output spatial filtering. The experimental nulls are limited by the effect of the spatial coherence properties of the source and the imperfect mode filtering on the output, but the fundamental physics of this technique have been demonstrated.

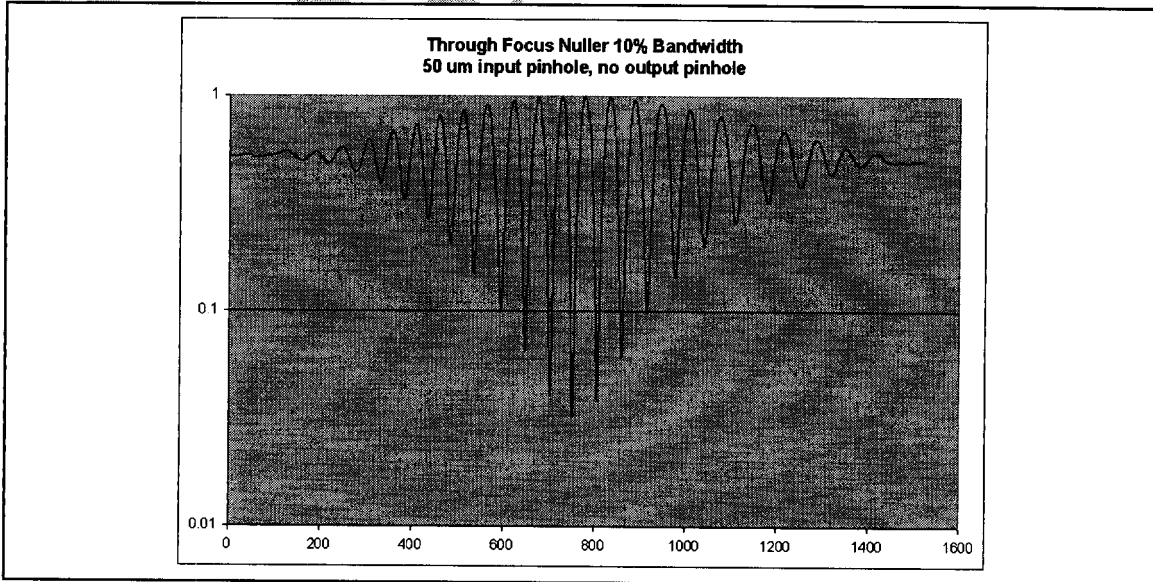


Fig. 6. Preliminary results from the through focus testbed.

2.4.4. Benefits/drawbacks of the through-focus architecture

The method, by its very nature, is broadband. In particular, if it were possible to develop a beamsplitter that covers the full TPF bandpass, then nulling could be done with a single device. However, producing a null even over a restricted portion of the band would give us great confidence in employing this method to cover the full band since most of the physics is captured by a handful of optics.

Polarization is a known problem with this method. We use the parabolas in an off axis configuration in order to give us an unobscured pupil. The angle of incidence varies across the pupil creates a pupil-dependent change in the s-p phase delay. These effects can be balanced, on average, by the angle of incidence on the flat mirrors of the straight through arm. It can also be minimized by a judicious selection of focal lengths and off-axis distances. But, it can never be eliminated.

The surface figure errors for powered surfaces can never be made to the same level as a flat surface. That and the alignment of these elements make it harder than a system completely composed of planar optics.

2.5. Periscope field flip

2.5.1. Description of the technique

In this architecture, the field flip is created by an inversion of the two pupils. This method has its roots in the rotational shearing interferometer. The original RSI showed great promise for nulling owing to its attractive polarization balancing properties, use of flat surfaces and simplicity. However, it was discovered that this technique has some asymmetry due to the addition of a compensating phase plate in one arm. It also suffered from diffraction effects from the spine of the rooftops (the location where the open-face rooftops make physical contact). Due to the geometric nature of the field flip, this architecture is also intrinsically achromatic. Thus a demonstration of this method over a portion of the 7-17 um band for TPF would give one great confidence that the other portions of the band could also be nulled with perhaps only a chance in the beamsplitter and compensator substrate.

2.5.2. Experiment description

Our latest version of the device removes these problems. It uses a pair of 90 fold mirrors (one 's' and one 'p' in each arm). The beam is split and combined in a novel way so as to match the path lengths in each arm. We implement it as a single beam Mach-Zehnder interferometer, and, by doing so, retain the benefits of a symmetric interferometer. Likewise, phase plates are added to remove the effects of residual dispersion due to differential glass thickness in the split and recombination beamsplitters.

We have initiated our laboratory testing with discrete components for the periscope elements that form the heart of this nulling arrangement. Eventually, they will be replaced with a single monolithic nulling periscope. This element because it is a single component, will keep the rooftops permanently aligned. The monolith will be made via optical contacting of four separate prisms to a base plate. All components will be coated simultaneously to insure the most homogeneous properties between them. This single component greatly simplifies the alignment since one only has to guarantee the shear and co-linearity of the two input beams, and matched angle-of-incidence on the output.

2.5.3. Benefits/drawbacks of this technique

Every surface in this configuration is planar, and is therefore easily fabricated to high quality. Perhaps the greatest difficulty with this method is that the input and output beams are non-coplanar. They are always perpendicular to each other. This could perhaps be mitigated with the addition of a couple of extra mirrors, but a system with the minimum number of surfaces is preferred.

3. Cryogenic Testing

3.1. Motivation

The ultimate, on-orbit environmental conditions will be quite different from those present in the aforementioned room-temperature test. The expected temperature is in the neighborhood of 40K. To

familiarize ourselves with the additional challenges of nulling at this temperature, we have a cryogenic-testing component of our activities. The testbed will examine survivability of components, opto-mechanical mounting, cryogenic actuation (both coarse and fine) and remote operation. However, the source and detectors will be at room temperatures. Therefore, flux from both the source and the background will be at levels much higher than those expected on orbit.

3.2. Experiment description

The layout for this system is shown in Fig. 7. It consists of three primary components: 1) the source, 2) the nulling interferometer (in cryogenic/vacuum environment) and 3) the detector assembly. We have decided upon the phase plate architecture for the initial tests. Only the interferometer will be exposed to the cryogenic environment, the other two will be at room temperature. Both the source/detector assembly breadboard and the nulling breadboard will be constructed to allow quick installation into the cryogenic chamber via a set of pillow blocks and rails. The rails are a part of the existing cryogenic/vacuum chamber. The initial setup and testing will be done on the same set of rails, but at room temperature. In this fashion, we hope to do a system level test of the hardware in order to save on the expense of debugging on the final system. Once all the benefits of room temperature operation has been exploited, all the hardware will move, en masse, to the cryogenic/vacuum facilities.

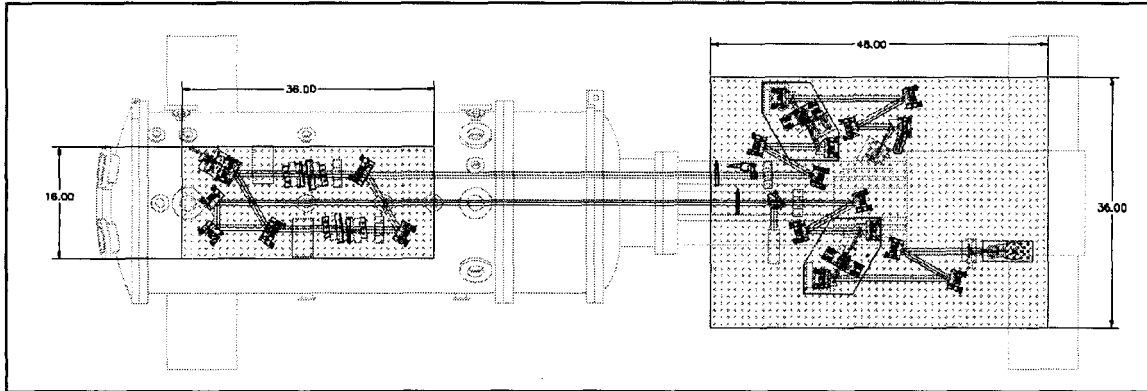


Fig. 7. Layout of cryogenic testing facility.

4. Enabling Technologies Development

4.1. Summary of areas of development

Although we have great confidence that nulling architectures we've chosen will allow us to demonstrate the principles of deep nulling, we still would be limited in our ability to measure if we didn't pursue a few, key, enabling technologies. These are: 1) a bright arc source, 2) laser metrology 3) active control 4) MIR detectors and 5) single mode spatial filters. The first four of these will be discussed in the following sections. The last will get a cursory treatment, owing to its development by another group at JPL. Our work to date has demonstrated that these ambitious nulling goals cannot be met unless there are satisfactory technical solutions to the above problems. These items cannot be ignored, and their importance cannot be minimized.

4.2. Arc Source

Broadband photons at 10 μ m are hard to get. A typical infrared thermal source operates at 1500K. Although it's possible to perhaps increase the temperature by a factor of two, the flux from say 8 to 12 μ m will only experience an increase of roughly a factor of two as well. Most of the increase in the total output is seen at shorter wavelengths. In order to increase the photon flux, the temperature must increase by a large factor: roughly 10,000 – 11,000 K for an order of magnitude increase (assuming the emissivity stays constant). In this vein, development of a bright white light source is key to our demonstration of deeper nulls.

Development of a novel arc source, based upon a source previously created at NIST, has been initiated. A typical arc source creates hot plasma between a pair of closely spaced electrodes. The plasma has an incredible temperature, but suffers from the lack of optical opacity. In our new source, two electrodes are

still used, but, as demonstrated by NIST, the novel configuration allows us to view the arc longitudinally, thereby overcoming the transparent nature of the arc when observed transversally.

Data from previously published data from the NIST source confirms that it does indeed act as a blackbody at 10,000K for wavelengths greater than $7 \mu\text{m}$. Some care must be taken in the use of such a source owing to the high current and voltage levels for the arc, and the creation of ozone. We expect to complete this source in about six months.

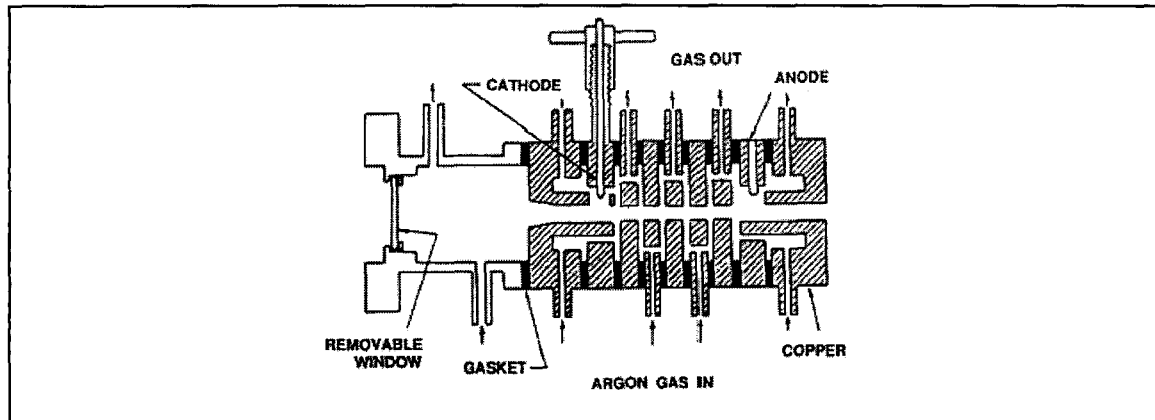


Fig. 8. Cross-section of the Argon arc source.

4.3. Laser metrology

Noise in the detection process can be mitigated by longer integration times to reduce detector noise. However, during this integration, drifts in the pathlength internal to the nulling interferometer will only bias the average null upwards. An increase in the averaging time only benefits if the internal path length will be maintained at a level so as not to degrade the null measurement.

Laser metrology for path length stability is the key. It has a long and rich history in stellar interferometry, but has only recently been used as a control error signal to stabilize the path length of a nulling interferometer. Our laser metrology gauge advances the field in a couple of ways. Our phase meter has matured such that it is implemented as a process running on a FPGA; we are cutting the ties to the existing hardware phase meter and its associated limitations. The new phasemeter also hosts the reference clock, so that no ancillary timing hardware is required. The integration of the reference clock simplifies the system, and provides an improvement in the temporal stability over the existing reference clock. It also provides for a higher reference frequency and therefore a proportionately higher single sample resolution of 0.2 nm with a heterodyne frequency of 100kHz.

4.4. Active Control

The nulling error budget contains several terms that require sensitive adjustment. To date, these have been done manually, and conditions have been created such that the need for active control is diminished. Terms that contribute to null degradation are: pupil shear and rotation, intensity mismatch, residual dispersion, piston instability and tip/tilt instability. The pupil alignments are slowly varying and can be corrected once, and verified infrequently. Intensity matching and residual dispersion require more frequent measurement and control between experiments. Finally, path length and tip/tilt control require monitoring and control during an experimental observation of deep nulls.

In order to better understand our control needs, we have created, what we call, an alignment storyboard. It consists of several scenarios, each scenario broken down into discrete steps. Broadly, they are, pupil alignment, tip/tilt alignment, intensity balance, fringe acquisition, residual phase measurement, and finally, the null measurement. In each step, the routine is to bring the step to a level that is quantifiable. This value is then compared to the amount deemed acceptable in the error budget. The system is actively controlled until it either moves onto the next step of the experimental observation sequence, or until it is unable to converge on the current step. The storyboard allows us to clearly identify all degrees of freedom, define the

update rates for the control system, give the components unique identifiers that can be agreed upon and documented. The document forms the foundation of all our discussions on our system control.

The control is implemented on a dual processor PC. One processor is dedicated to the real-time tasks, the other is charged with the mundane, non-deterministic processes associated with the operating system. These non-real time tasks include graphical display of the real-time routines. The system is inexpensive, with the real time costs only a fraction of the cost of a development seat on a VME system. The PC architecture opens a broad avenue of hardware options that is otherwise a limited in more historic real-time implementations such as VME.

The most challenging requirement for the real-time system is that of laser metrology and closed-loop path-length control. Our system has demonstrated the ability to sample the laser metrology at 10kHz and close the loop, using the laser metrology as the error signal, at 1kHz. On similar nulling testbed at JPL, the Planet Detection Testbed, the result was a residual path length stability of sub 1 nm rms.

4.5. Detector Development

Detector noise limits our measurement at the bottom of the fringe. We are therefore developing a more sensitive method of measuring the lowest null signals, while also covering the full dynamic range of the null signal. A single pixel of a arsenic-doped silicon (Si:As) blocked-impurity band (BIB) array is considered by many to be the detector of choice. A cryogenic-dewar is currently under contract to meet these needs. The dewar shall provide the additional task of bandpass filter selection, dispersion control, and spatial mode filtering. It is currently on contract and we expect it before February of 2005.

4.6. Single-mode spatial filters

The single-mode spatial filter development activity is being done by another group at JPL. This discussion will be brief. It is meant to convey the need for these devices, and then to give a brief outline of our current options. The benefits of a single mode filter to nulling interferometry are well documented in the literature. Such devices do not exist to that cover the whole 7-17 um wavelength range that is baseline for TPF. For technology demonstrations we have a restricted optical bandwidth of only 20%. Several methods are under consideration at this point. They are: 1) integrated optics, 2) polycrystalline Silver Halide, and 3) chalcogenide glasses.

These devices not only serve as mode filters on the output of the system, they likewise are used to create a spatially coherence source on the input side. The devices are essential in our efforts to demonstrate deep nulls. We expect to have a working device in hand by the end of the calendar year.

5. Cryogenic Nulling

The ultimate means of building confidence in our understanding of the requirements for nulling for TPF is to construct an experiment that approximates the conditions as it will be during observation. The experiment we've envisioned will demonstrate rudimentary planet detection at the faint TPF-like fluxes for both the star and planet at TPF-like cryogenic temperatures (40K) with a null depth of 10^{-5} (and null stability of 10^{-6}) at an optical bandpass of 50% for long periods of time (~2 hours).

Our preliminary design work for such a cryogenic nulling experiment is shown below. It employs a double sided breadboard with the source injection on one side, and the nulling interferometer on the opposite side. The path length and tip/tilt metrology will proceed from source to detector and is therefore non-TPF-like.

CONCLUSION

Three different nulling architectures are being pursued to demonstrate the challenging requirements of nulling at the 10^{-6} level with a 20% bandwidth. These room-temperature tests will occur simultaneously with initial cryogenic nulling tests that will demonstrate the fundamentals of nulling operations in the cryogenic environment. Results from these tests feed the ultimate test of the nulling for TPF. This system will demonstrate rudimentary planet detection, with simulated stellar and planetary fluxes that are traceable to those expected on orbit.

We are well on our way to demonstrating the requisite nulling levels for a the planned TPF-I Mission.

ACKNOWLEDGMENTS

This work was carried out by the Jet Propulsion Laboratory, California Institute of Technology, under contract with the National Aeronautics and Space Administration and supported by the Terrestrial Planet Finder Program – TPF.

REFERENCES

1. B. Mennesson, et. al., 2002, Optical Planet Discoverer: How to Turn a 1.5 m Telescope into a powerful exo-planetary systems imager, *Proc. SPIE*,
2. D. Liu, et. al. 2003, Design and fabrication of a coherent array of single-mode optical fibers for the nulling coronagraph, these proceedings.
3. M. Shao, et. al. 2003, Planet detection in visible light with a single-aperture telescope and nulling coronagraph, these proceedings.
4. R. M. Morgan, J. Burge, & N. Woolf, "Achromatic phase control using refractive materials", *Proc. SPIE* 4006, 340, 2000.
5. J. Kent Wallace, G. Hardy, and E. Serabyn, "Deep and stable interferometric nulling of broadband light with implications for observing planets around nearby star", *Nature*, **406**, 700.
6. E. Serabyn and M. Colavita, "Symmetric Beam Combiners for Nulling Interferometry", *Applied Optics*, **40**, 1668.
7. E. Serabyn, *Proc. SPIE*, 4006, 328, 2000.
8. B. Mennesson, M. Ollivier and C. Ruiller, "Single-mode waveguides to correct the optical defects of a nulling interferometer", *J. Opt. Soc. Am.*, **19**, 3, 596.
9. J. W. Brault, "Fourier Transform Spectrometry", *Proc. 15th Adv. Course in Astr. & Astrophysics*, Huber, Benz & Mayor, eds., (1985).